Revista Mexicana de Física **40**, *No. 2 (1994) 175–187*

Laser-material interactions; fundamentals and applications*

N. BLOEMBERGEN
Pierce Hall, Harvard University
Cambridge, MA 02138, USA

Recibido el 6 de noviembre de 1993; aceptado el 11 de noviembre de 1993

ABSTRACT. The interaction of light with matter leads to electronic excitation by the absorption of photons. A large fraction of the high excitation energy of the electrons is transformed into heat on a time scale of about one picosecond in many circumstances. With lasers, power flux densities or intensities exceeding a terawatt/cm^2 are readily achieved and any material may be converted into a high temperature plasma. The material response has been investigated over a wide range of intensities and irradiation times. Applications include heat treatment and ablation of surfaces, cutting, drilling and welding of a wide variety of materials, laser recording and printing, and laser surgery. Phase transitions induced by ultrashort femtosecond laser pulses enlarge our understanding of materials under extreme conditions of pressure and temperature.

RESUMEN. La interacción de luz con materia conduce a excitaciones electrónicas por la absorción de fotones. En muchas circunstancias, una fracción importante de la energía de alta excitación de los electrones se transforma en calor en una escala de tiempo de aproximadamente un picosegundo. Usando láseres se consiguen fácilmente densidades o intensidades de flujo de potencia por encima de terawatt/cm^2 y cualquier material se puede convertir en un plasma de alta temperatura. La respuesta del material se ha investigado en un amplio rango de intensidades y tiempos de irradiación. Las aplicaciones incluyen el tratamiento por calor y ablación de superficies, el corte, taladro y soldado de una amplia variedad de materiales, el grabado e impresión por láser y la cirugía. Las transiciones de fase inducidas por pulsos ultrarrápidos de láser de algunos femtosegundos incrementan nuestra comprensión de los materiales en condiciones extremas de presión y temperatura. (*Traducción de los editores.*)

PACS: 34.80.Qb

1. INTRODUCTION

The sun at the zenith on a clear day irradiates the surface of the earth with a power flux density of 0.14 watts/cm^2. Such an exposure makes us feel uncomfortably hot. When sunlight is concentrated by a converging lens or mirror materials may be heated to three thousand degrees or more. Large-scale solar furnaces have existed for decades. It was already known in Greek antiquity that sunlight concentrated by a spherical flask with transparent liquid could ignite dry sticks of wood [1]. When the Phoenician fleet beleaguered the harbor of Syracuse in 212 B.C. Archimedes proposed to set fire to the rigging of the enemy ships by having soldiers use their shiny shields to concentrate the sunlight onto them.

*This work was supported in part by Joint Services Electronic under Contract NOOO14-89-J-1023. It was presented in a public lecture at UNAM on 8 November 1993.

With lasers it is straightforward to obtain much higher flux densities. Consider, for example, a one watt argon ion laser. The diffraction limited beam could be focused to a spot size of 10^{-8} cm^2 by a microscope objective lens, leading to a continuous wave power flux density of 10^8 watts/cm^2. With a powerful 10 kW cw CO_2 laser a flux density of 10^4 watts/cm^2 can be achieved on an area of 1 cm^2 virtually without focusing. This flux density is roughly equal to the flux density prevailing at the surface of the sun, *i.e.*, black-box radiation of about 6000 K.

In addition to concentration in space, light fluxes may be concentrated in time. In pulsed Q-switched and mode-locked lasers, pulse durations in the range of 10^{-8} to 10^{-11} seconds are readily achieved. Consider a small Nd-Yag laser delivering 100 millijoules of light energy per pulse. If this light is emitted in 10^{-11} s and focused onto a spot 1 mm in diameter, a power flux density of 10^{12} watts/cm^2 is obtained. One terawatt, or 10^{12} watts, roughly equals the total power output of all electric power plants on earth. Imagine this power concentrated on 1 cm^2. One obtains flux densities comparable to those prevalent in the interior of stars, corresponding to blackbody radiation at 10^6 K.

It is clear that absorption of laser light leads to very rapid heating of opaque materials to very high temperatures. Melting, evaporation and high temperature plasma formation may occur. The high temperature conditions may be quite localized in space and time.

In the next section the fundamental processes of light absorption will be outlined. The basic interaction mechanisms in metals, in semiconductors and in materials that are optically transparent at low light intensities will be reviewed. Different behavior depending on a wide range of power flux densities and interaction times (or pulse durations) will be described.

The fundamental scientific ideas of laser interactions were developed in the decade immediately following the realization of the first laser in 1960. Readers who wish more details should consult a monograph, published in 1971, which contains many references to early, original literature [2]. A more recent review of laser-material interactions may be found in a study which considered the action of high power lasers as weapons [3].

Section 3 describes various important applications based on the fundamental effects. Representative examples are taken from laser printing and recording, from laser surgery and from metalworking. The time scale, the power flux density and the utilized laser wavelength depend strongly on the technological objective.

Section 4 is devoted to the interaction with very short light pulses of picosecond or femtosecond duration(10^{-11} to 10^{-14} s). On these shortest time scales local thermodynamic equilibrium is not assured. Interesting phenomena associated with phase transitions on this time scale are reviewed. Production of high-temperature, high-density plasma is achieved on these time scales at power flux densities in the range of 10^{12} to 10^{18} W/cm^2. Section 5 contains a brief summary.

2. FUNDAMENTAL PROCESSES

The primary process is electronic excitation by the absorption of a photon, if the material is absorbing at low light intensities. In metals the dominant absorption mechanism involves free-free transitions. A conduction electron increases its kinetic energy by the

energy of the photon $h\nu$, while momentum balance is maintained by the simultaneous collision with another particle, for example an ion core. The process is known as "inverse bremsstrahlung" because bremsstrahlung is the process of radiation when an electron is scattered during a collision and consequently loses kinetic energy. The absorption causes the temperature of the conduction electron gas to rise. By electron-phonon interaction, the absorbed energy is transferred in part to the motion of the atoms or ions making up the metallic lattice. Typical transfer times between hot electrons and the lattice are on the order of one picosecond for most materials. The heating by free-free transitions is usually well described by a Drude model. The highly collisional electron plasma has a short electronic relaxation time τ_e. This leads to an effective high-frequency conductivity, which describes the reflectivity as well as the penetration depth of the transmitted light. Usually visible light penetrates a distance of 3×10^{-6} to 10^{-5} cm into the metal. In this thin layer the initial heat production takes place. Thermal conduction will carry heat deeper into the metal. The penetration depth by heat conduction is on the order of $\sqrt{\kappa t_p}$, where κ is the thermal diffusivity and t_p is the duration of the irradiation. The thermal conductivity κ lies between 0.1 and 1 cm^2/s for most metals. Heat diffuses between 1 mm to 1 cm in one second, as we know from stirring a hot cup of tea with a metal spoon. For $t_p \sim 10^{-10}$ s the diffusion length is comparable to the penetration or absorption depth of the light in metals.

In semiconductors the photon energy must exceed the band gap in order to have significant absorption. The basic process is now the creation of an electron-hole pair, corresponding to a transition of an electron from the valence to the conduction band. The electrons and holes may have a considerable kinetic energy $h\nu - E_g$. This energy is rather rapidly shared with the lattice vibrations and leads again to heating of the semiconductor material, again on a time scale of picoseconds. In intense laser pulses the density of electrons may become so high, that rapid electron-hole recombination occurs via Auger processes, *i.e.*, the other carriers take up the recombination energy E_g as well. In this case the behavior of semiconducting materials becomes rather similar to that of metals.

Insulating materials, with $h\nu \ll E_g$, are optically transparent. At very high radiation intensities multiphoton processes become sufficiently probable, that significant concentrations of conduction electrons are created. When this happens the subsequent heating mechanisms become again rather similar to those described for metals and semiconductors.

This rather coarse description does not do justice to the vast amount of details that solid state physics has amassed about the structure, thermal and electronic properties of thousands of materials. Striking differences depending on details of electronic structure are evident in spectroscopic studies at low intensity. The global effects of high excitations; to which this review is limited, are rather similar for many materials. Significant laser heating leads to melting, evaporation and plasma formation of all targets.

For excitation with power flux densities exceeding 10 kW/cm^2 heat losses at the surface due to radiation and convective cooling may be ignored. The power flux density of blackbody radiation is given by Stefan-Boltzmann law, σT^4, and corresponds to 1 kW/cm^2 at $T = 3644$ K, a temperature above the boiling point of most materials. Convective cooling by air-flow over a 3000 K surface at a Mach number unity amounts to only a few

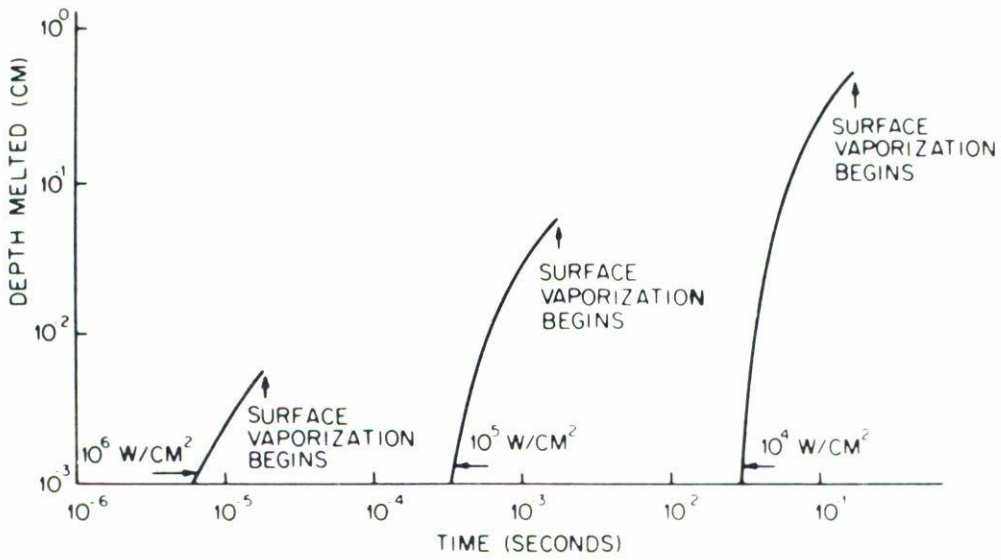

FIGURE 1. Melted depth in yellow brass as a function of time for various laser flux densities (after J.F. Ready [2]).

hundred W/cm^2. Thus the absorbed energy from laser radiation serves basically to heat the material. Assume that both the laser spot size r_0 and the material thickness d_0 are large compared to the diffusion length $(\kappa t_p)^{1/2}$. In this case the temperature rise $T - T_0$ at the surface may be estimated from

$$(\kappa t_p)^{1/2} \rho C_v (T - T_0) \approx (I - R) I_0 t_p, \tag{1}$$

where ρ is the density, C_v the specific heat per unit volume, R the reflectivity and I_0 the laser intensity. Figure 1 shows the time it takes for the surface of yellow brass to reach the boiling point for various laser power flux densities. It also shows the depth to which the sample is melted.

The time for melt-through t_m of a sample of thickness d_0, assuming that the liquid materials is removed by gravity or by a convectional shear flow may be estimated from

$$(I - R) I_0 t_m = \rho d_0 [C_v (T_M - T_0) + L_M], \tag{2}$$

where T_M is the melting temperature and L_M is the latent heat of melting. With $R = 0.8$ for aluminum at a certain wavelength and $d_0 = 0.5$ cm, one finds a time for melt-through $t_m = 0.65$ s at $I_0 = 10$ kW/cm^2. In the early days a ruby laser pulse of 1 Joule, of 1 ms duration and of about 1 mm diameter could punch holes through a number of razor blades. The strength of the pulse was measured in the unofficial units of "gillettes". The steady-state rate of evaporation from thick target may be estimated from the energy condition

$$(I - R) I_0 = \dot{m} H_c(g). \tag{3}$$

Here H_c is the enthalpy of the gas phase and the rate of mass removal per unit area, $\dot{m}$ is also related to the surface temperatures T by

$$\dot{m} = M_0 N(T_s)\langle v_z \rangle \simeq \frac{p(T_s)}{(2\pi k T_s M_0)^{1/2}}. \tag{4}$$

Here $p(T_s)$ is the vapor pressure at the temperature T_s, $N(T_s)$ the corresponding number density of atoms or molecules with mass M_0 in the vapor. Equations (3) and (4) determine the temperature T_s the surface assumes under steady-state conditions. Carbon has one of the largest values of $H_c(g)$, the heat of evaporation. According to Eq. (3), a protective heat shield containing 1 g/cm^2 of carbon, with $H_s = 32$ kJ/g would be evaporated in about 3 seconds for $I_0 = 10$ kW/cm^2, assuming $R < 0.1$. These simple examples give us an estimate of laser capabilities. More elaborate calculations give details about the temperature distribution inside the sample, the influence of radial heat diffusion from small laser spots, the variation of reflectivity, heat conductivity and specific heat with temperature, etc.

The most important modifications arise at high fluences from the fact that the vapor in front of the surface becomes sufficiently dense and ionized, such that the laser radiation is significantly absorbed by the plasma [4]. The target material becomes decoupled from the laser radiation, but may in turn be reheated by UV radiation from the plasma. Additional chemical reactions may take place, if the target is not bounded by vacuum but is placed in air or another atmosphere. If the target is initially highly reflecting for laser light, a localized plasma blob may be formed by the evaporation of an absorbing dust particle. the localized heated plasma will in turn heat its surroundings by UV radiation which is not strongly reflected by the target. Thus the coupling between target and the laser beam is enhanced in this case. Plasma effects are usually important in the range 10^6 W/cm^2 < $I_0 < 10^{10}$ W/cm^2. For $I_0 > 10^{10}$ W/cm^2 about 1 J/cm^2 of energy gets delivered in 10^{-10} s. In this time interval the heat diffusion length is less than the absorption depth which is assumed to be 10^{-5} cm. The energy gets deposited in a layer about 10^{-5} cm thick. A straightforward estimate shows that this layer, regardless of the nature of the substance gets heated to 10^4 K or higher, well above the critical point. The material is thus rapidly transformed into a high temperature, high density plasma. This regime will be considered in Sect. 4. The next section deals with large-scale practical applications of lasers at flux densities below 10^8 W/cm^2.

3. Applications of laser-materials interactions

One of the earliest large-scale technological applications is laser printing. An argon-ion laser with a cw output of 1 to 10 watts may be focused to a spot with a diameter of about 10 μm. Consider a mylar sheet coated with a film, about 0.5 μm thick, of metallic aluminum or chromium. The considerations of the previous section show that a hole in the metallic film is created by evaporation in less than 1 μs. The laser spot can be scanned rapidly and modulated in intensity to cut a pattern in the film. Since the metal and mylar

present different adhesive properties for a printing dye, laser fabrication of printing plates is achieved.

Information can also be recorded by laser spots with a linear dimensions of 1 μm, comparable to the optical wavelength, onto photoresist material. The light produces in this case a change in electronic linkages, rather than a temperature change. Subsequent chemical etching records each bit of information on an area of 10^{-8} cm^2. This process is used in the recording of compact disks. One CD has a storage capacity of 10^{11} bits, sufficient to record the entire *Encyclopædia Britanica*. The information is read with a small infrared semiconductor laser ($< 10^{-4}$ W), which senses the phase difference of the reflection from the etched surface.

It is also possible to record information on magnetic tapes by means of lasers. The magnetized tape is put into an external magnetic field with reverse bias. The magnetic anisotropy prevents domain rotation and flipping of the magnetization. When the laser focal spot heats a domain closer to the Curie temperature the magnetization will flip. The bits of laser-recorded information can in principle be read out by a low power polarized light beam, as the polarization of the reflected light depends on the state of magnetization.

Argon-ion lasers are also used to heat living tissues in the human body. The light gets primarily absorbed by red blood cells. An early application was the repair of detached retinas by creating scar tissue. The laser beam passes through the eye ball without doing harm, because it is not yet focused and the eye fluids are transparent. The beam gets focused on the retina where cells in blood vessels are evaporated and an exposure of suitably short duration prevents damage to the surroundings charred. Thus many tiny spots of scar tissue may be formed to repair retinal tears or even pan-retinal detachment which often occurs in severe diabetes cases.

The laser treatment of port-wine stains provides another example where differential absorptivity of living tissue plays a crucial role. The birthmark is caused by an abnormal high concentration of tiny blood vessels in the skin, separated by normal tissue. It is possible to adjust the intensity and the pulse duration of the argon laser such that the areas with excess blood vessels get heated in the temperature range of 50°–90°C. The proteins in these cells coagulate (compare boiling of an egg) and the cells are killed. The normal regions in between do not reach the temperature of 50°C and remain alive. Careful timing depends of course on the knowledge of the typical dimensions and heat conductivity of the healthy tissue between blood vessels.

In photodynamic therapy, certain porphyrin dyes are introduced into the body. These dyes may be preferentially absorbed by cancerous tissues. Laser irradiation at wavelength near the maximum dye absorption may be used to preferentially kill cancer cells.

The radiation of CO_2 lasers near 10 μm wavelength is strongly absorbed by all water containing tissue. They can be used to evaporate diseased tissue, for example of the liver, without causing hemorrhages, as the blood vessels at the edge of the treated area are cauterized.

Laser beams in the near infrared, or at shorter wavelength, can be focused to a spot size of 1 μm, or they can be channeled into an optical fiber of dimensions of a few μm. Such spots rapidly evaporate tissue and can make cuts that are sharper than the best metallic surgical scalpel can produce. Many new surgical procedures have been developed, using

a variety of lasers. Invasive procedures are minimized, as the light beam can be steered to inaccessible locations by endoscopes and optical fibers.

As an example of the precision which is attainable by laser treatment, let us consider the interaction of an XeF excimer laser pulse with a human hair. It is possible to ablate 1 μm per pulse and to drill a hole through the hair. Such pulses may also be used to drill a hole through industrial diamonds, used in wire drawing processes.

With such pulsed laser the power level is sufficiently high that plasma effects may become important in the ablation process. A recent detailed quantitative study was carried out with excimer laser pulses on copper [4]. Both ArF at $\lambda = 193$ nm and XeF at $\lambda = 351$ nm were used with a pulse duration of about 10^{-8} s. The power flux density was varied from 0.1 to 1.2 G/cm^2 and the energy fluence covered the range from 1 to 12 J/cm^2. Four steps could be distinguished. First evaporation occurs, leading to thermal etching of the copper surface. Next multiphoton ionization in the copper vapor takes place. Electron heating and electron-atom collision induce further ionization, resulting in spark-like breakdown of the vapor. In the final step energy is transported from the plasma back to the Cu sample, resulting in plasma etching.

Laser cutting is also widely used in the textile industry. Cutting patterns may be programmed by movable mirrors and a clean cut may be produced in any material. The trimming of ceramic components, *e.g.*, resistors and capacitors in the electronics component industry is also an important application. Silicon crystal wafers are implanted with ions (boron or phosphorus) to obtain *p*-type and *n*-type layers for the fabrication of diode junctions and transistors. After ion implantation the crystalline structure is damaged. With pulsed laser heating the implanted layer may be annealed quickly, without appreciable thermal diffusion of the implanted impurities. Thus sharp *np*-type junctions are obtained in near perfect single crystal wafers.

There is a general trend to replace most lower power gas lasers with more rugged and less expensive semiconductor lasers. These also have a much longer lifetime. Semiconductor laser arrays with an output exceeding one watt are being developed. Up conversion of the semiconductor laser to the visible by harmonic generation in integrated solid state devices is also possible.

The most powerful cw lasers are the CO_2 lasers near 10 μm wavelength and the hydrogen fluoride chemical lasers in the mid-infrared range. The former are used on a large scale in the heavy metal working industry, which utilizes CO_2 lasers with outputs between 5 and 25 kW. They are used to cut steel beams or butt-weld two beams several inches thick. The automotive industry uses them for chassis fabrication and for surface heat treatment of metal parts. For example, the surfaces of gears or the cylinder walls of a combustion engine should be hardened to reduce wear from friction. With mirrors and a CO_2 laser beam it is possible to rapidly heat and cool (quench) the surfaces only, avoiding brittleness of the bulk material. Lasers are also used to drill cooling channels near the tips of titanium fan blades to improve the efficiency of jet turbine engines. The potential of such high power lasers as military weapons has been considered from the very beginning of laser development. In addition to CO_2 lasers, chemical lasers (HF and DF) have been constructed with a cw power output exceeding one megawatt. Their possible use in strategic defense against intercontinental missiles has been analyzed [3]. The idea of deployment of such directed energy weapons was abandoned after considerable public

debate several years ago, well before the end of the cold war. Tactical laser weapons are, however, a military reality.

4. ULTRASHORT PULSES AND ULTRAHIGH IRRADIANCES

Consider the case that the absorption depth, $d_{\text{abs}} = \alpha^{-1}$, the reciprocal of the absorption coefficient, is comparable to or larger than the heat diffusion length, $d_{\text{abs}} > (\kappa t_p)^{1/2}$. For times larger than the electron-phonon energy relaxation time, $t_p > \tau_e$, local thermodynamic equilibrium may be assumed. In this case all of the laser energy is deposited in the absorption depth and the average temperature rise of this layer may be estimated from

$$C_v(T - T_0)d_{\text{abs}} = (1 - R)\int_0^{t_p} I_0\, dt. \tag{5}$$

It is proportional to the energy fluence in the laser pulse. The melting point of any strongly absorbing material can be reached at modest fluences. For example, tungsten melts at a fluence of 0.1 J/cm^2 at $\lambda = 1.06$ μm in a 30 ps pulse. Silicon melts at 0.2 J/cm^2 in a 20 ps pulse at $\lambda = 0.53$ μm. On melting the reflectivity changes abruptly to the value characteristic of molten silicon [5]. At the same time the absorption depth at $\lambda = 0.53$ μm changes from 2×10^{-5} cm to 3×10^{-6} cm. Experimental data for the reflectivity of silicon at several wavelengths as a function of the fluence in a pump pulse preceding the probe by 15 ps is shown in Fig. 2. The changes in reflectivity below the melting point are due to the creation of an electron-hole plasma. The maximum carrier density of about 6×10^{20} is reached at 0.1 J/cm^2 corresponding to a plasma frequency in the near infrared. Extensive investigations have been made of the heating of the electrons in metals and of the plasmas created in semiconductors as a function of pump fluence, wavelength, and time delay after the pump pulse.

The interest here is, however, focused on the effect of fluences above the melting threshold. If the fluence exceeds this threshold by a factor three to five the surface layer of most material will attain temperatures above the boiling point and even the critical point. The estimated surface temperature of silicon heated by very short pulse of 1 J/cm^2 is 6000 K. With a power flux density of 10^{12} W/cm^2 it is possible to heat materials to temperatures exceeding 10^4 K in less than a few picoseconds. Thus a thin layer of a highly ionized plasma at the original target density is created. This fluid at extremely high temperature and pressure will commence to expand in a rarefaction wave [6]. The front of the material will travel with a velocity [6,7]

$$v_{\max} = \frac{2}{\gamma - 1} v_0 = \frac{2}{\gamma - 1}\left(\frac{ZkT_e}{M_0}\right)^{1/2}. \tag{6}$$

Here v_0 is the sound velocity in the plasma. The electron temperature is T_0 and M_0 is the mass of the ions with charge Ze, while γ is the ratio of the specific heats at constant pressure and volume, respectively. For $\gamma = 5/3$, the front velocity exceeds the sound velocity by a factor 3, and the kinetic energy of the particles at the front, which escape

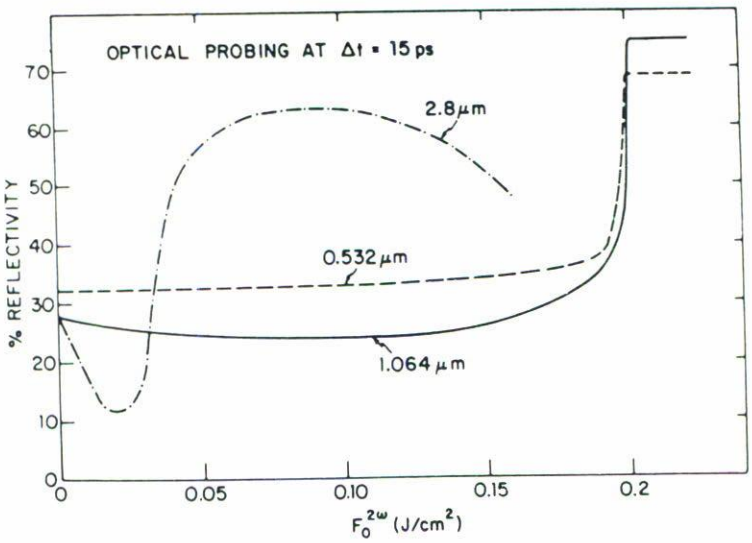

FIGURE 2. The reflectivity of crystalline silicon at three different wavelengths, 15 ps after pump pulse 0.53 μm, as a function of pump fluence (after Ref. [5]).

normal to the surface, may exceed the thermal kinetic energy by an order of magnitude. This has been observed. For $T_e = 10^4$ K and $M_0 = 28 \times 10^{-24}$ g for silicon one finds $v_{max} = 3 \times 10^5$ cm/s. A plasma layer of 3×10^{-6} cm initial thickness expands to twice this value in 10^{-11} s. On this time scale the boundary becomes diffuse.

The gradient in density and the concomitant gradient in optical index of refraction acquire a length scale equal to a significant fraction of the optical wavelength, approaching $1/4\lambda$. Consequently the reflectivity will drop. This drop in reflectivity at fluences of 1 J/cm^2 and more in silicon has been observed with picosecond pulses. Experiments carried out with femtosecond pulses can probe the plasma expansion more precisely, as will be described later. A large body of work, extending over the past three decades and still continuing, is concerned with the creation of high temperature plasmas. Thermonuclear fusion processes have been demonstrated in laser produced low Z plasmas (isotopes of hydrogen). The long-range goal is of course energy production by controlled thermonuclear fusion. A small spherical sample of hydrogen gas is irradiated isotropically by a number of laser beams at fluences exceeding 10^{14} W/cm^2. In less than a picosecond a dense plasma has been created at the expense of less than one percent of the laser pulse energy. The bulk of the laser pulse is used to heat and compress this plasma further. The compression of the core occurs because of momentum reaction from the expansion of an outgoing spherical rarefaction wave. Extensive computational codes have been developed to describe the energy transfer between the laser and the inhomogeneous plasma blob, which lie beyond the scope of this overview [8].

High Z, high temperature plasmas created by short intense laser pulses are effective sources of continuum X-ray radiation. Over fifty percent of the laser pulse energy may be converted to blackbody X-radiation. With care an X-ray laser medium may be produced [9]. Amplification of an X-ray line at 20.6 and 20.9 nm wavelength was convincingly demonstrated in a plasma created by the evaporation of selenium film. A 75 nm thick Se

film was deposited on a 150 nm thick Formvar substrate. The foil was 1.1 cm long and illuminated at $\lambda = 0.53$ μm by a line focus from a cylindrical lens with a spot size of 0.02×1.12 cm. The nominal pulse length was 450 ps, and the typical incident intensity was 5×10^{13} W/cm^2. The plasma created from the exploding foil contains Neon-like Se^{24+} ions. A population inversion is established between the $2p^5 3p$ and the $2p^5 3s$ transitions, based on the differential rates for collisional creation and radiative decay. Extensive computational codes for details of plasma evolution and composition have been developed. This subject is, however, outside the scope of this review, which concentrates on the initial steps in the conversion of condensed matter by rapid heating to very high temperatures.

Finally, we turn to the interaction with femtosecond pulses. For $t_p < 10^{-13}$ s, there is no time for the energy acquired by the electronic system to be shared with the heavier particles (atoms) constituting the lattice $t_p < \tau_e$. The interactions between electrons are usually fast enough to warrant the assumption of a local electron temperature. Anisimov [10] first discussed a regime with different electron and lattice temperatures. If the fluence in the focused femtosecond pulse is sufficiently high, say exceeding 0.1 J/cm^2, hot carrier densities in semiconductors exceeding 10^{22}/cm^3 may be created. In metals the conduction electron gas is heated well above 10^4 K and becomes nondegenerate. On a time scale τ_e, which usually lies in the range between 10^{-13} and 10^{-12} s, the hot electrons share their kinetic energy with the atoms. On a time scale more than a few picoseconds after the irradiation by the pump pulse we are back to the regimes discussed above. At the end of the femtosecond pulse a situation has been created of a very hot electron plasma at the original solid density, while the atoms are still cold. They are essentially in their original lattice positions as they have not had time for significant displacement in 10^{-14} s. The concept of lattice bonds is, however, lost as the electrons are so highly excited. Estimates have been made for a tetrahedral structure of silicon, that if more than ten percent of the valence electrons are promoted from bonding to antibonding orbitals, the electronic structure collapses [11]. The electrons make a phase transition to a plasma.

The hot electron plasma will expand, but can only do so by pulling atoms along to conserve overall neutrality. Since the bonding forces of the original lattice structure have already been eliminated, the fluid excited layer will commence to expand as a rarefaction wave described by Eq. (6).

A number of femtosecond pump and probe experiments on semiconductors and metals support this picture. The reflectivity of silicon following irradiation by a strong femtosecond pulse was observed [12] as function of time over tens of picoseconds with a resolution of 0.1 ps. The silicon surface melts over a circular area, but the reflectivity of the central area decreases after a few picoseconds because of material expansion in the rarefaction wave of this area which has been heated above the critical point.

The weak second harmonic generation by quadrupole interaction in the silicon crystals shows a distinctive anisotropy, related to the crystalline orientation a the surface [13]. This second harmonic radiation is only created during the femtosecond pulse. The anisotropy disappears rather abruptly above a threshold fluence level. The electronic structure has apparently made a transition to an isotropic plasma phase.

The second harmonic generation in GaAs is even more revealing [14,15]. Here the SH generation is electric dipole allowed because the lattice structure lacks inversion symmetry. The pump pulse polarization and the crystal can be so oriented that it does not create SH.

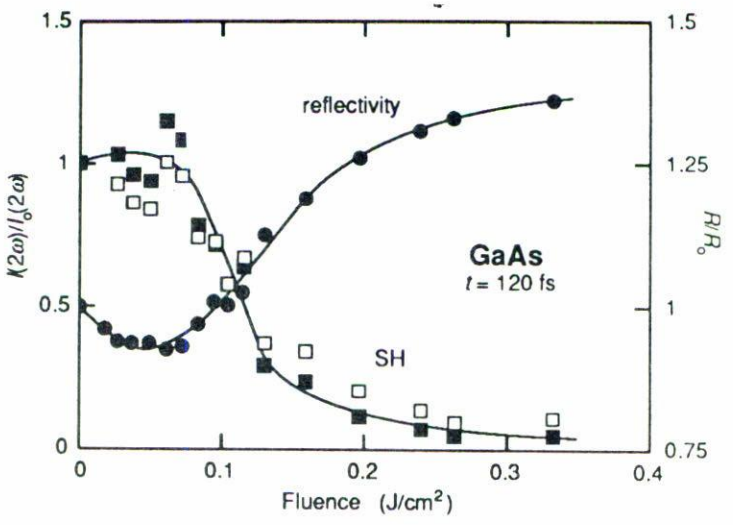

FIGURE 3. Fluence dependence of the reflected second harmonic intensity (solid squares) and reflectivity (round dots) of a (110) GaAs surface. The data were taken at 120 fs delay with 100 fs pulses at 620 nm wavelength at an incident angle of 45°. The open squares are the second harmonic divided by $[(1-R)/(1-R_0)^2]$ to correct for changes in reflectivity (after Ref. [14]).

The SH created by the probe pulse can be monitored as a function of pump fluence and time delay. Simultaneously the change in reflectivity can be monitored. The experimental results in Fig. 3 show the existence of a sharp fluence threshold above which the SHG by the probe pulse drops by a factor ten. It essentially vanishes within the experimental error [14]. This happens in less than 10^{-13} s. This time is shorter by at least factor five than the known interaction time between energetic electrons and optical phonons in this crystal. Thus we have evidence for a purely electronic phase transition from a structure with oriented bonding orbitals to a structure with inversion symmetry, presumably a nearly isotropic plasma. The rise and subsequent decay of the reflectivity is also consistent with the formation of a dense plasma and its subsequent expansion. Previously, the changes in SHG and in reflectivity of GaAs as a function of fluence have been measured with pulses of 20 ps deviation. There the expected result could be explained by ordinary melting of the lattice to a liquid metallic phase [16].

Very detailed investigations have recently been carried out on phase transitions induced in graphite and diamond by femtosecond pulses [17]. An increase and subsequent rapid decrease in the reflectivity is observed, following irradiation by a femtosecond pump pulse of 90 fs duration at $\lambda = 620$ nm above a threshold value. This threshold is 0.13 J/cm^2 for highly-oriented pyrolytic graphite and 0.63 J/cm^2 for a diamond crystal. The diamond must first become absorbing by multiphoton processes. The sudden increase in reflectivity indicates an electronic phase transition to a high density plasma. Its optical properties are described rather well by a Drude model with $\omega_p \tau_e \sim 1$. The decrease in reflectivity is due to plasma expansion which creates a boundary layer with an index gradient. At an angle of incidence of 50° there is a marked difference in the behavior of s- and p-polarized light in this transition layer. Detailed investigations of the reflection of a probe pulse over a wide wavelength range, a wide range of pump fluences, both above [17] and below threshold [18],

and with time delay resolution of 100 fs, yield a wealth of information about the state of carbon at extremely high pressure and temperature. It is believed that in highly excited graphite the electrons and atoms thermalize in about 0.5 ps. After this time a state of fluid carbon has been created, which may be characterized as quasi-metallic.

Heating of metallic aluminum by femtosecond pulses and measuring the reflectivity as a function of incident fluence has permitted measurement of the resistivity [7] up to electron temperatures of 10^6 K. The self-reflectivity of 5 mJ 0.4 ps pulses at $\lambda = 300$ nm from aluminum has been measured up to intensities of 10^{15} W/cm^2. Careful analysis of the data must again take account of plasma expansion during the 0.4 ps time interval. The resistivity reaches a maximum at a temperature $T_e \sim 40$ eV. Then the resistivity decreases as $T_e^{-3/2}$ characteristic of a high temperature plasma. Other metals may be analyzed in a similar manner.

5. CONCLUSION

A broad survey of laser-materials interaction shows a variety of regimes, depending on the power flux density and time of irradiation. For densities not exceeding 10^6 W/cm^2 ordinary heating, melting and evaporation describe the majority of effects. Many practical applications are based on this regime. At intensities above 10^6 W/cm^2 plasma effects in the evaporated material become important. Plasmas drastically influence the coupling with the substrate. At intensities above 10^{10} W/cm^2, in strongly absorbing materials a layer of 30 to 300 nm thickness gets heated to the melting temperature or higher on a time scale of 10^{-10} s or less. Any material may be transformed rapidly into a high density, high temperature plasma. Details of the initiation of the plasma heating of the electrons and of electron-phonon interactions are accessible to experimental investigation. With femtosecond pulses phase transitions in the electronic structure have been demonstrated. Initially a condition of a hot dense electron plasma with cold atoms and ions in their original lattice configuration is created. The subsequent evolution can be studied. The investigation of the optical properties of materials on a femtosecond time scale and the behavior of atoms and molecules at intensities from 10^{14} to 10^{18} W/cm^2 will remain an active and fruitful field of endeavor in the coming decade.

REFERENCES

1. Aristophanes, *Comedy of the Clouds*, 421 B.C. English translation, B.B. Rogers, 1955, Doubleday, New York.
2. J.F. Ready, *Effects of High-power Laser Radiation*, Academic Press, New York (1971).
3. "Report of the APS Study Group on the science and technology of directed energy weapons", edited by N. Bloembergen and C.K.N. Patel, *Rev. Mod. Phys.* **59** (1987) S1-S201.
4. R.W. Dreyfus, *J. Appl. Phys.* **69** (1991) 1721.
5. N. Bloembergen in *Beam-Solid Interactions and Phase Transformations*, edited by H. Kurz, G.L. Olson and J.M. Poate, Elsevier North-Holland, (1986) *Mat. Res. Soc. Symp. Proc.* **51** (1985) 3.
6. Y.B. Zel'dovich and Yu. P. Raizer, *Physics of Shock Waves and High-Temperature Hydrodynamic Phenomena*, Vol. 1, Ch. 1, Academic Press, New York (1966).

7. H.M. Milchberg, R.R. Freeman, S.C. Davey and R.M. More, *Phys. Rev. Lett.* **61** (1988) 2364.
8. See, for example, M.C. Richardson, R.S. Craxton, J. Delettrez, R.L. Keck, R.L. McCrory, W. Seka and J.M. Soures, *Phys. Rev. Lett.* **54** (1985) 1656 and references quoted therein.
9. M.D. Rosen, P.L. Hagelstein, D.L. Matthew, E.M. Campbell, A.U. Hazi, B.L. Whitten, B. MacGowan, R.E. Turner, R.W. Lee, G. Charatis, G.E. Busch, C.L. Shepard and P.D. Rockett, *Phys. Rev. Lett.* **54** (1985) 106; D.L. Matthew, P.L. Hagelstein, M.D. Rosen, M.J. Eckart, N.M. Ceglio, A.U. Hazi, H. Medecki, B.J. MacGowan, J.E. Trobes, B.L. Whitten, E.M. Campbell, C.W. Hatchez, A.M. Hawryluk, R.L. Kauffman, L.D. Pleasance, G. Rambach, J.H. Segfield, G. Stone and T.A. Weaver, *Phys. Rev. Lett.* **54** (1985) 110; S. Suckewer, C.H. Skinner, H. Milchberg, C. Keane and D. Voorhees, *Phys. Rev. Lett.* **55** (1985) 1753.
10. I. Anisimov, B.L. Kapeliovich and T.L. Perelman, *Sov. Phys. JETP* **39** (1974) 375.
11. J.A. van Vechten, R. Tsu and F.W. Saris, *Phys. Lett.* **74A** (1979) 422 and references quoted therein.
12. M.C. Downer, R.L. Fork and C.V. Shank, *J. Opt. Soc. Am.* **B2** (1985) 595.
13. H.W.K. Tom, G.D. Aumiller and C.H. Brito-Cruz, *Phys. Rev. Lett.* **60** (1988) 1438.
14. P. Saeta, J.K. Wang, Y. Siegal, N. Bloembergen, and E. Mazur, *Phys. Rev. Lett.* **67** (1991) 1023.
15. T. Schröder, W. Rudolph, S.V. Govorkov and I.I. Shumai, *Appl. Phys.* **A51** (1990) 49.
16. J.M. Liu, A.M. Malvezzi and N. Bloembergen, *Appl. Phys. Lett.* **49** (1986) 622; N. Bloembergen, A.M. Malvezzi and J.M. Liu, *Appl. Phys. Lett.* **45** (1984) 1019.
17. D.H. Reitze, H. Ahn and M.C. Downer, *Phys. Rev.* **B45** (1992) 2677; D.H. Reitze, X. Wang, H. Ahn and M.C. Downer, *Phys. Rev.* **B40** (1989) 11986.
18. K. Seibert, G.C. Cho, W. Kütt, H. Kurz, D.H. Reitze, J.I. Dadap, H. Ahn, M.C. Downer and A.M. Malvezzi, *Phys. Rev.* **B42** (1990) 2842.